

Single Defect Centers in Diamond Nanocrystals as Quantum Probes for Plasmonic Nanostructures

Andreas W. Schell,^{a*} Günter Kewes,^a Tobias Hanke,^b
Alfred Leitenstorfer,^b Rudolf Bratschitsch,^b Oliver Benson^a
and Thomas Aichele^a

^a Humboldt-Universität zu Berlin, Institute of Physics,
Newtonstraße 15, D-12489 Berlin, Germany

^b University of Konstanz, Department of Physics and Center for Applied
Photonics,

Universitätsstraße 10, D-78464 Konstanz, Germany

*andreas.schell@physik.hu-berlin.de

Abstract. We present two applications of a single nitrogen vacancy center in a nanodiamond as quantum probe for plasmonic nanostructures. Coupling to the nanostructures is achieved in a highly controlled manner by picking up a pre-characterized nanocrystal with an atomic force microscope and placing it at the desired position. Local launching of single excitations into a nanowire with a spatial control of few nanometers is demonstrated. Further, a two dimensional map of the electromagnetic environment of a plasmonic bowtie antenna was derived, resembling an ultimate limit of fluorescence lifetime nanoscopy.

Defect centers in diamond have proven to be excellent quantum light sources. They are active at room temperature, do not photobleach and have long spin decoherence times even at room temperature [1]. In particular the nitrogen vacancy (NV) center [2, 3] has been widely studied to realize single photon emitters [4, 5] or nanophotonic elements [6], to implement quantum information processing [7], and to optically detect magnetic fields with nanometer spatial resolution [8, 9]. The latter publications have introduced NV centers as optical nanoprobe. NV centers in diamond nanocrystals are particularly useful for this application due to their small size of less than a few 10 nanometers [10]. STED microscopy with NV centers for example provides an optical resolution of 6 nm [11]. The role of an optical nanoprobe can be twofold. First, it can create a well defined optical excitation which is then launched into a nearby system under investigation [12]. The generation of a single photon from an NV center can thus be regarded as an ultimate quantum limit of a pump pulse in a pump-probe experiment. Second, the probe itself can respond to a change of its local environment which can then be monitored optically. Key requirements for a local quantum probe are stability, since only a weak signal is created, and the ability to position the probe with excellent spatial precision. In this paper we demonstrate how NV centers in single nanodiamonds can be utilized as quantum probes to study plasmonic nanostructures.

Surface plasmons polaritons (SPPs) [13] concentrate electromagnetic fields in volumes much smaller than the optical wavelength. This can be exploited to enhance light-matter interaction and to modify the emission characteristics of light emitters. However, due to the strong confinement sub-wavelength probing is mandatory if such

structures shall be characterized satisfactorily. In a first experiment, we utilize the nanodiamond quantum probe to study propagation of SPPs along metal nanowires [14]. Propagation loss, as well as input/output efficiency are crucial parameters for applications of SPP waveguides in novel miniaturized photonic components [15, 16]. In the following we study SPPs on the level of single quanta. In previous experiments, excitation of single surface plasmon states by a single NV center and guiding along a metal nanowire was demonstrated using structures which were randomly assembled by deposition of metal nanowires and quantum emitters on a sample surface [17, 18, 19, 20]. Therefore, on-demand positioning and change of a once assembled configuration was not possible.

In our experiments, we use a setup consisting of a confocal microscope combined with an atomic force microscope (AFM) (see Fig. 1(a)). This combination allows both optical detection of photons and nanomanipulation of the nanodiamond probes [21, 22]. Photon correlation measurements were performed with a Hanbury-Brown and Twiss (HBT) configuration of two avalanche photo diodes (APDs, quantum efficiency at 700 nm approximately 30 %). A diamond nanocrystal containing a single NV defect center and thus resembling a quantum probe was first optically characterized on a coverslip and then individually picked up by the AFM tip. Then, the nanocrystal was transferred to a coverslip with chemically synthesized silver nanowires and placed on-demand near a previously selected wire which served as SPP waveguide. With this technique one can be sure that there is exactly one diamond containing exactly one single NV defect center on the whole sample. So there is no possibility of accidentally measuring photons coming from a diamond containing more than one defect center. Nanomanipulation with the AFM tip then allowed positioning of the nanocrystal and launching of a single excitation at arbitrary positions along the wire.

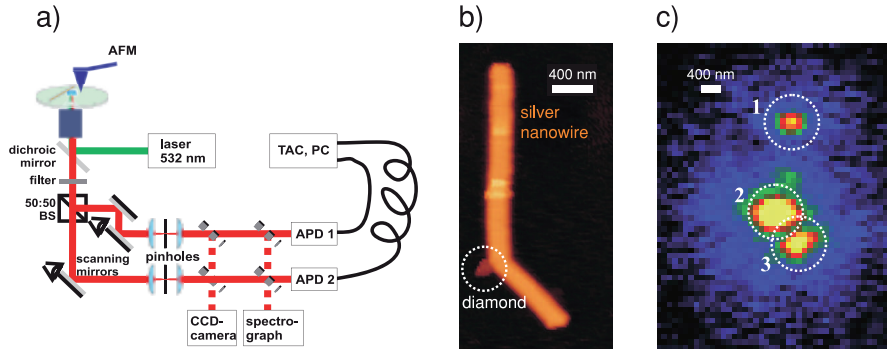


Figure 1. Coupling of a diamond nanocrystal with a single NV center to a silver nanowire and excitation of single surface plasmon polaritons. (a) Scheme of the experimental setup. (b) AFM image of the diamond nanocrystal (indicated by the dashed circle) positioned at the side of a bent silver nanowire. (c) Microscope photoluminescence image of the same configuration. Positions 1 and 3 indicate the ends of the nanowire, while position 2 marks the location of the diamond nanocrystal.

Fig. 1(b) shows an AFM image of the nanowire, which has a diameter of ≈ 80 nm. A sharp bend separates the nanowire into two arms of $1.9 \mu\text{m}$ and $0.7 \mu\text{m}$ length. Under continuous wave laser excitation of the NV center (at a wavelength of 532 nm), photoluminescence directly from the diamond nanocrystal (position 2 in Fig. 1(c)) as well as light emerging from the bend and from the ends of the nanowire (positions 1

and 3 in Fig. 1(c)) are visible. Since there is a strong fluorescence background emerging from the bend of the nanowire while exciting the diamond, for further measurements the diamond was placed at another position, so that the nanowire bend is no longer in the excitation spot (position 2 in Fig. 2(c)). Already this repositioning of the nanocrystal shows the advantage of nanomanipulation. Accidental inconvenient configurations can be corrected and experiments can be repeated under otherwise unchanged conditions. At the same time, the ability to reposition is crucial in more complex structures, since slight changes of the position of an emitter with respect to a plasmonic structure may already modify its emission as well as the structures plasmonic properties significantly. Despite the possibility to perform near-field simulations, under experimental conditions an a priori prediction of an optimum position for an emitter or nanoprobe is often impossible [23].

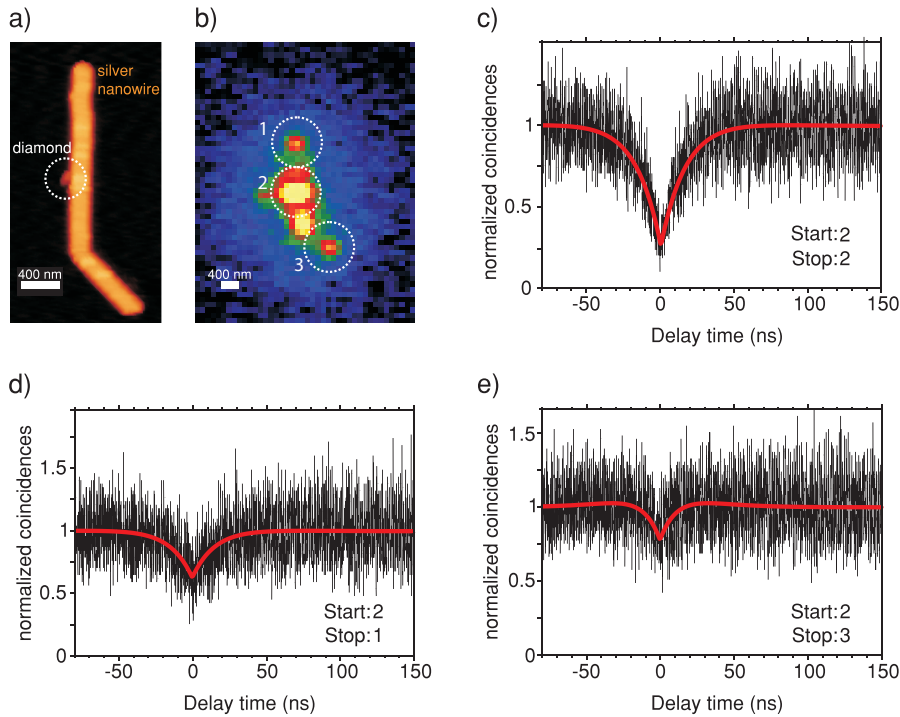


Figure 2. A nanodiamond probe launching single plasmonic excitations. (a,b) AFM and fluorescence image showing a silver nanowire and a nanodiamond with a single NV center. The bright spot between position 2 and 3 in (b) emerges from the bend of the nanowire. (c) Autocorrelation of the photons from the diamond measured at point 2. (d,e) Cross-correlations between the photons emitted from position 2 and from positions 1 and 3, respectively. The anti-bunching dip in the curves clearly reveals the non-classical properties.

With the new position of the diamond nanocrystal there are now four fluorescent spots observable on the nanowire. One (position 2 in Fig. 2(b)) corresponds to the emission of fluorescence directly from the nanodiamond. An autocorrelation measurement on this spot shows a pronounced anti-bunching behavior (Fig. 2(c)), confirming the single photon character of emission from a single NV center in the nanodiamond. The other spots now correspond to three output ports for single

excitations launched into the wire via the nanodiamond quantum probe. In order to prove the quantum nature of the excitations we performed cross-correlation measurements between the light directly emitted from the nanodiamond (position 2 in Fig. 2(b)) and the light emitted from both ends of the nanowire (positions 1 and 3, respectively, in Fig. 2(b)). Again, a clear anti-bunching was observed proving that indeed light from the quantum probe was converted into single plasmonic excitations which propagated to the output ports. The nanowire thus represents a plasmonic beamsplitter with three output ports, a key building block for quantum plasmonic elements. When generating plasmons from the excitation of a single quantum emitter anti-bunching after reconversion to photons is expected. However, we would like to point out that the preservation of a pronounced anti-bunching dip is an excellent indicator to quantify the contribution of unwanted stray light and background fluorescence which may occur in complex plasmonic structures. The single nanodiamond is also a perfect test probe for this purpose.

In another experiment with optical antennas we exploit the second feature of the nanodiamond probe, i.e. its ability to map the local electromagnetic environment of a plasmonic nanostructure.

A plasmonic antenna is highly desired in experiments on the level of single quantum emitters as it excites the quantum emitter efficiently, extracts many photons out of the quantum emitter, and spatially directs the emitted photons towards a specific direction [24, 25, 26]. We investigated gold bowtie antennas fabricated with electron-beam lithography on a glass substrate with our nanodiamond probe. In contrast to a configuration where the antenna is decorated with several emitters in a purely random manner [27], we utilize again AFM nanomanipulation. In this way we control the position of the nanodiamond with nanometer precision, i.e. we investigate a large number of different emitter/antenna configurations, using exactly the same constituents [28]. A mapping of the electromagnetic environment via observing the optical properties of the nanoprobe is thus possible.

In the experiment we used the setup shown in Fig. 1(a), but with another excitation laser operating at 10 MHz pulsed excitation at 532 nm wavelength. All measurements (except the power dependence) were performed at an power of 40 μ W at the back of the slightly overfilled NA=1.35 oil immersion objective.

There are different processes when coupling an emitter to a plasmonic antenna. The excitation as well as the radiative rate are enhanced, but additional non-radiative decay channels may open up [29]. Also the modified spatial emission pattern may change the number of the detected photons on a detector of finite solid angle [30]. In our spatial mapping we determined the lifetime of the NV center's excited state and the total enhancement of the photon emission rate. By repeatedly measuring the lifetime and changing the nanodiamond's position with the AFM (see Fig. 3(a-f)) we obtained the lifetime maps depicted in Fig. 4 (a,b). The lifetimes were measured via time correlated single photon counting. In order to suppress short-lived emission from the gold, count events within the first few nanoseconds were not taken into account for the fitting to theoretical decay curves (see Fig. 3 (g,h)).

The antennas were fabricated to have a gap of 10 nm and consist of two isoscele triangles with an altitude that equals the short side of 140 nm (Fig. 4(a)) and 150 nm (Fig. 4(b)). This geometries give a fundamental mode in the infra-red. In Fig. 4(a) a diamond with a height of approximately 60 nm and an oval shape was used, which was too large to fit in the antenna gap. The exact position of the NV center in this nanodiamond has therefore also an a priori uncertainty of approx. 60 nm. For this

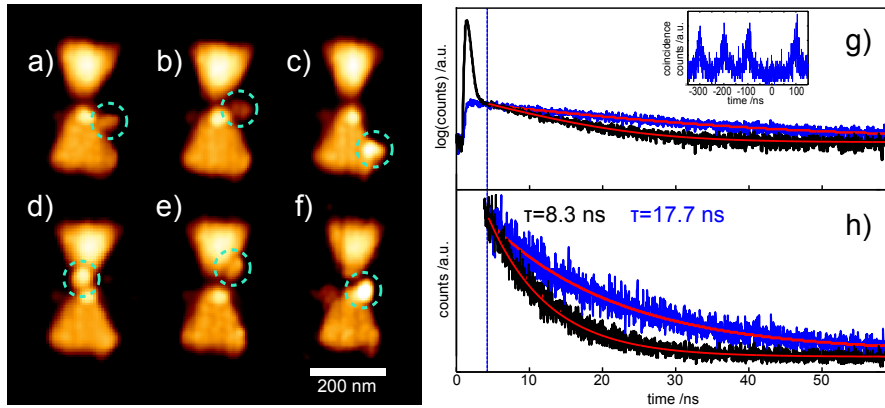


Figure 3. (a-f) Aligning a nanodiamond probe. A single nanodiamond was moved with the AFM to different positions with respect to a bowtie antenna. Small changes in the measured topography are due to changes of the AFM tip's shape during the manipulation process. Circles highlight the positions of the nanodiamond. (g,h) Fluorescence lifetime histogram of a uncoupled nanodiamond (blue) and the nanodiamond coupled to a bowtie antenna (black). The initial peak stems from short-lived fluorescence from the gold of the bowtie antenna, which our detectors could not resolve. Only counts occurring 3 ns after the emission peak (indicated by the blue vertical line) are used to fit (red curves) the fluorescence decay from the NV center in the nanodiamond. Inset in (g) shows the coincidences for the uncoupled diamond measured with the HBT setup.

reason in the measurements depicted in Fig. 4(b) we used a nanodiamond of 15 nm height to reduce these problems. The two-dimensional maps in Fig. 4 resemble an ultimate limit of fluorescence lifetime nanoscopy, having only one quantum emitter present.

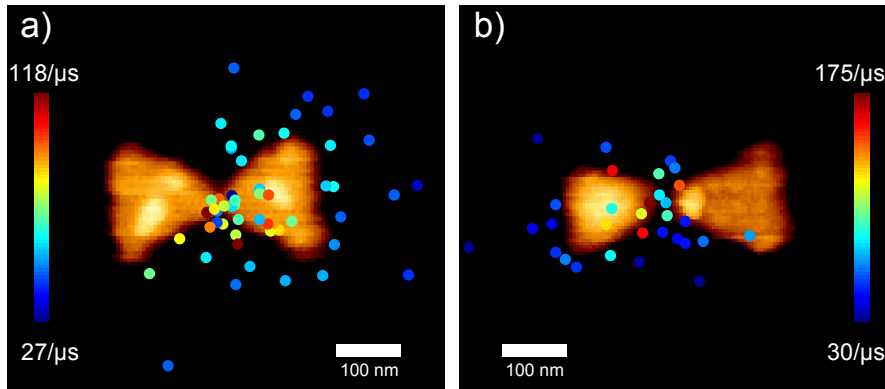


Figure 4. (a,b) Maps showing the decay rate of the excited state of the NV center in the nanodiamond probe for different positions with an underlay of the corresponding AFM image of the antennas. In (a) a diamond of approx. 60 nm height and an oval shape was used. In (b) the diamond height was about 15 nm.

Beyond the mapping of the electromagnetic environment of the antenna our data provides information about the actual enhancement of the fluorescence rate of the NV center in the nanodiamond. For a quantitative analysis, we compared the uncoupled

diamond to the situation where the nanodiamond is coupled to the antenna in an optimum position. We placed the nanodiamond in the antenna gap, where also an excellent alignment of the diamond with respect to the excitation laser spot is possible. The uncoupled diamond has a lifetime of $\tau_u = 17.7$ ns, which is reduced to $\tau_c = 8.3$ ns when the diamond is in the antenna gap. Also the photon emission rate from the diamond is changed from $R_u = 2.5$ kHz to $R_c = 2.2$ kHz. The reduction is due to additional loss channels which open up close to the metal surface. However, care has to be taken in the analysis since we perform pulsed excitation at a fixed excitation rate and a single NV center only can get excited once per cycle, if the duration of the excitation pulse is small compared to the NV center's lifetime. Due to coupling to the antenna both radiative and non-radiative decay is enhanced, i.e. the lifetime of the excited state is significantly shortened. This means that although the probability of generating a photon after excitation is reduced, photons can be provided in principle at a much higher rate.

The key number is the rate of photon emission under continuous saturated excitation, which could be calculated from the emission's power dependence under pulsed excitation. Since we observed melting of the gold nanoantennas at an excitation power of ca. 50 μ W, which is clearly below the saturation intensity, it was not possible to determine the enhancement factor with adequate accuracy.

In summary, we have shown that a single NV center in a nanodiamond can act as stable quantum probe working at room temperature. Together with a controlled AFM manipulation ultimate limits of pump-probe experiments can be performed, where the pump consists of only a single excitation launched with nanometer spatial precision into the structure under investigation, in this case a plasmonic beamsplitter. At the same time two-dimensional maps of plasmonic antenna structures can be derived. These maps provide insight into the near-field properties of antenna structures allowing optimization of the designs [31]. The method of repeatedly repositioning the quantum emitter and mapping the lifetime can in principle be extended to almost any system of interest, if they are accessible with an AFM [6, 5].

We thank Ulrike Woggon for providing the silver nanowires and the DFG project IQuOSuPla for financial support.

- [1] T. A. Kennedy, J. S. Colton, J. E. Butler, R. C. Linares, and P. J. Doering, "Long coherence times at 300 k for nitrogen-vacancy center spins in diamond grown by chemical vapor deposition," *Appl. Phys. Lett.* **83**, 4190–4192 (2003).
- [2] F. Jelezko and J. Wrachtrup, "Single defect centres in diamond: A review," *phys. stat. sol. (a)* **203**, 3207–3225 (2006).
- [3] R. Brouri, A. Beveratos, J.-P. Poizat, and P. Grangier, "Photon antibunching in the fluorescence of individual color centers in diamond," *Opt. Lett.* **25**, 1294–1296 (2000).
- [4] C. Kurtsiefer, S. Mayer, P. Zarda, and H. Weinfurter, "Stable solid-state source of single photons," *Phys. Rev. Lett.* **85**, 290–293 (2000).
- [5] T. Schröder, A. W. Schell, G. Kewes, T. Aichele, and O. Benson, "Fiber-integrated diamond-based single photon source," *Nano Lett.* **11**, 198–202 (2010).
- [6] J. Wolters, A. W. Schell, G. Kewes, N. Nüsse, M. Schoengen, H. Doscher, T. Hannappel, B. Löchel, M. Barth, and O. Benson, "Enhancement of the zero phonon line emission from a single nitrogen vacancy center in a nanodiamond via coupling to a photonic crystal cavity," *Appl. Phys. Lett.* **97**, 141108 (2010).
- [7] T. D. Ladd, F. Jelezko, R. Laflamme, Y. Nakamura, C. Monroe, and J. L. O'Brien, "Quantum computers," *Nature* **464**, 45–53 (2010).
- [8] G. Balasubramanian, I. Y. Chan, R. Kolesov, M. Al-Hmoud, J. Tisler, C. Shin, C. Kim, A. Wojcik, P. R. Hemmer, A. Krueger, T. Hanke, A. Leitenstorfer, R. Bratschitsch, F. Jelezko,

- and J. Wrachtrup, "Nanoscale imaging magnetometry with diamond spins under ambient conditions," *Nature* **455**, 648–651 (2008).
- [9] J. R. Maze, P. L. Stanwix, J. S. Hodges, S. Hong, J. M. Taylor, P. Cappellaro, L. Jiang, M. V. G. Dutt, E. Togan, A. S. Zibrov, A. Yacoby, R. L. Walsworth, and M. D. Lukin, "Nanoscale magnetic sensing with an individual electronic spin in diamond," *Nature* **455**, 645–648 (2008).
- [10] Y. Sonnefraud, A. Cuche, O. Faklaris, J.-P. Boudou, T. Sauvage, J.-F. Roch, F. Treussart, and S. Huant, "Diamond nanocrystals hosting single nitrogen-vacancy color centers sorted by photon-correlation near-field microscopy," *Opt. Lett.* **33**, 611–613 (2008).
- [11] E. Rittweger, K. Y. Han, S. E. Irvine, C. Eggeling, and S. W. Hell, "Sted microscopy reveals crystal colour centres with nanometric resolution," *Nat. Phot.* **3**, 144–147 (2009).
- [12] A. Cuche, O. Mollet, A. Drezet, and S. Huant, "'Deterministic' quantum plasmonics," *Nano Letters* **10**, 4566–4570 (2010).
- [13] W. L. Barnes, A. Dereux, and T. W. Ebbesen, "Surface plasmon subwavelength optics," *Nature* **424**, 824–830 (2003).
- [14] H. Ditlbacher, A. Hohenau, D. Wagner, U. Kreibig, M. Rogers, F. Hofer, F. R. Aussenegg, and J. R. Krenn, "Silver nanowires as surface plasmon resonators," *Phys. Rev. Lett.* **95**, 257403 (2005).
- [15] Z. Li, K. Bao, Y. Fang, Y. Huang, P. Nordlander, and H. Xu, "Correlation between incident and emission polarization in nanowire surface plasmon waveguides," *Nano Lett.* **10**, 1831–1835 (2010).
- [16] M. W. Knight, N. K. Grady, R. Bardhan, F. Hao, P. Nordlander, and N. J. Halas, "Nanoparticle-mediated coupling of light into a nanowire," *Nano Lett.* **7**, 2346–2350 (2007).
- [17] R. Kolesov, B. Grotz, G. Balasubramanian, R. J. Stohr, A. A. L. Nicolet, P. R. Hemmer, F. Jelezko, and J. Wrachtrup, "Wave-particle duality of single surface plasmon polaritons," *Nat. Phys.* **5**, 470–474 (2009).
- [18] A. V. Akimov, A. Mukherjee, C. L. Yu, D. E. Chang, A. S. Zibrov, P. R. Hemmer, H. Park, and M. D. Lukin, "Generation of single optical plasmons in metallic nanowires coupled to quantum dots," *Nature* **450**, 402–406 (2007).
- [19] Y. Fedutik, V. V. Temnov, O. Schöps, U. Woggon, and M. V. Artemyev, "Exciton-plasmon-photon conversion in plasmonic nanostructures," *Phys. Rev. Lett.* **99**, 136802 (2007).
- [20] H. Wei, D. Ratchford, X. E. Li, H. Xu, and C.-K. Shih, "Propagating surface plasmon induced photon emission from quantum dots," *Nano Letters* **9**, 4168–4171 (2009).
- [21] M. Barth, N. Nüsse, B. Löchel, and O. Benson, "Controlled coupling of a single-diamond nanocrystal to a photonic crystal cavity," *Opt. Lett.* **34**, 1108–1110 (2009).
- [22] S. Schietinger, M. Barth, T. Aichele, and O. Benson, "Plasmon-enhanced single photon emission from a nanoassembled metaldiamond hybrid structure at room temperature," *Nano Lett.* **9**, 1694–1698 (2009).
- [23] D. E. Chang, A. S. Sørensen, P. R. Hemmer, and M. D. Lukin, "Quantum optics with surface plasmons," *Phys. Rev. Lett.* **97**, 053002 (2006).
- [24] P. Mühlischlegel, H.-J. Eisler, O. J. F. Martin, B. Hecht, and D. W. Pohl, "Resonant optical antennas," *Science* **308**, 1607–1609 (2005).
- [25] O. L. Muskens, V. Giannini, J. A. Sánchez-Gil, and J. Gómez Rivas, "Strong enhancement of the radiative decay rate of emitters by single plasmonic nanoantennas," *Nano Lett.* **7**, 2871–2875 (2007).
- [26] R. Esteban, T. V. Teperik, and J. J. Greffet, "Optical patch antennas for single photon emission using surface plasmon resonances," *Phys. Rev. Lett.* **104**, 026802 (2010).
- [27] A. Kinkhabwala, Z. Yu, S. Fan, Y. Avlasevich, K. Müllen, and W. E. Mörner, "Large single-molecule fluorescence enhancements produced by a bowtie nanoantenna," *Nat. Phot.* **3**, 654–657 (2009).
- [28] J. Merlein, M. Kahl, A. Zuschlag, A. Sell, A. Halm, J. Boneberg, P. Leiderer, A. Leitenstorfer, and R. Bratschitsch, "Nanomechanical control of an optical antenna," *Nat. Phot.* **2**, 230–233 (2008).
- [29] J. N. Farahani, D. W. Pohl, H.-J. Eisler, and B. Hecht, "Single quantum dot coupled to a scanning optical antenna: A tunable superemitter," *Phys. Rev. Lett.* **95**, 017402 (2005).
- [30] A. G. Curto, G. Volpe, T. H. Taminiau, M. P. Kreuzer, R. Quidant, and N. F. van Hulst, "Unidirectional emission of a quantum dot coupled to a nanoantenna," *Science* **329**, 930–933 (2010).
- [31] M. D. Wiersma, A. W. Schell, K. S. Ilin, M. Siegel, and H.-J. Eisler, "Nanoengineering and characterization of gold dipole nanoantennas with enhanced integrated scattering properties," *Nanotechnology* **20**, 425203 (2009).